Polarization and Differential Cross Section for Neutrons Scattered from ^{12}C †

R. O. Lane

Ohio University, Athens, Ohio and Argonne National Laboratory, Argonne, Illinois 60439

AND

R. D. Koshel

Ohio University, Athens, Ohio

AND

J. E. Monahan

Argonne National Laboratory, Argonne, Illinois 60439

(Received 7 August 1969)

The polarization $P(\theta)$ and differential cross section $\sigma(\theta)$ for the scattering of neutrons of $0.1 \leq E_n \leq 2.0$ MeV from ^{12}C have been measured at five or nine angles. $P(\theta)$ contains a slowly varying $\sin\theta$ term and is dominated by a negative $\sin 2\theta$ term which grows strongly with energy so that $P(120°)$ reaches as much as 40% at higher energies. The experimental values of $\sigma(\theta)$ and $P(\theta)$ are simultaneously described reasonably well over this energy range in terms of a two-level R-function formalism. Anomalous background effects are estimated by use of a square-well interaction potential.

I. INTRODUCTION

MOST of the information regarding the interaction of low-energy neutrons with ^{12}C has come from measurements of total cross sections,[1-5] capture cross sections,[6] differential scattering cross sections,[7-10] and from a few measurements of polarizations.[11] Since the capture cross section at low energies has been shown[6] to be only a few millibarns, the scattering of neutrons from ^{12}C has frequently been used as a convenient and reliable secondary standard of flux calibration. Measurements of the total cross section have been interpreted[5,12] chiefly in terms of s-wave scattering which predominates at low energies. Some early measurements[7] of the differential scattering cross section $\sigma(\theta)$ indicated, within experimental error, that $\sigma(\theta)$ was isotropic in the c.m. system up to 1.5 MeV, where p-wave contributions begin to be evident. Our early measurements[8,10] of $\sigma(\theta)$ showed a small but definite fore-aft p-wave asymmetry at somewhat

lower energies, and this asymmetry slowly increased with energy. In a general survey experiment[11] of the polarization of neutrons scattered at 90°(lab) and 45°(lab), appreciable polarization was observed even as low as $E_n \approx 0.7$ MeV. This confirmed the presence of higher-order partial waves, and further showed that they were spin-dependent.

The work described here is a much more complete study of both $P(\theta)$ and $\sigma(\theta)$, measured simultaneously at either 5 or 9 angles, for a large number of energies up to 2 MeV. These data are used to determine the parameters in the R-matrix description[13] of the scattering. The representation in terms of R-matrix parameters facilitates comparison with the results of more detailed shell-model, coupled-channel, and cluster-type calculations. These measurements show that $P(\theta)$ reaches as high as 40% at certain angles, and an understanding of these relatively large polarizations in terms of the states in ^{13}C makes ^{12}C attractive as an analyzer for polarization experiments. A brief preliminary report[14] of these results has been given.

II. EXPERIMENT

The apparatus and the analysis connected with the present experiment have been described in earlier papers.[8,10,11,14,15] The reaction ^{7}Li$(p, n)^7$Be provided a partially polarized beam of neutrons emitted at 51°

† Work performed under the auspices of the U. S. Atomic Energy Commission and the Ohio University Fund.

[1] D. W. Miller, Phys. Rev. **78**, 806 (1950).

[2] C. K. Bockelman, D. W. Miller, R. K. Adair, and H. H. Barschall, Phys. Rev. **84**, 69 (1951).

[3] C. Kimball, J. E. Monahan, and F. P. Mooring, Argonne National Laboratory Report No. ANL-5894, p. 28, 1958 (unpublished).

[4] C. M. Huddleston, R. O. Lane, L. L. Lee, Jr., and F. P. Mooring, Phys. Rev. **117**, 1005 (1960).

[5] K. K. Seth, E. G. Bilpuch, and H. W. Newson, Nucl. Phys. **47**, 137 (1963).

[6] J. H. Gibbons, R. L. Macklin, and J. H. Neiler, Phys. Rev. **122**, 182 (1961).

[7] H. B. Willard, J. K. Bair, and J. D. Kington, Phys. Rev. **98**, 669 (1955).

[8] A. Langsdorf, Jr., R. O. Lane, and J. E. Monahan, Phys. Rev. **107**, 1077 (1957).

[9] J. E. Wills, J. K. Bair, H. O. Cohn, and H. B. Willard, Phys. Rev. **109**, 891 (1958).

[10] R. O. Lane, A. Langsdorf, Jr., J. E. Monahan, and A. J. Elwyn, Ann. Phys. (N.Y.) **12**, 135 (1961).

[11] A. J. Elwyn and R. O. Lane, Nucl. Phys. **31**, 78 (1962).

[12] R. G. Thomas, Phys. Rev. **88**, 1109 (1952).

[13] A. M. Lane and R. G. Thomas, Rev. Mod. Phys. **30**, 257 (1958).

[14] R. O. Lane, A. J. Elwyn, F. P. Mooring, J. E. Monahan, and A. Langsdorf, Jr., Bull. Am. Phys. Soc. **12**, 1185 (1967).

[15] Previous publications that describe experiments in which the spin-precession magnet was used are R. O. Lane, A. J. Elwyn, and A. Langsdorf, Jr., Phys. Rev. **126**, 1105 (1962); A. J. Elwyn, R. O. Lane, and A. Lansdorf, Jr., *ibid.* **128**, 779 (1962); A. J. Elwyn, R. O. Lane, A. Langsdorf, Jr., and J. E. Monahan, *ibid.* **133**, B80 (1964); R. O. Lane, A. J. Elwyn, and A. Langsdorf, Jr., *ibid.* **133**, B409 (1964); **136**, B1710 (1964); Nucl. Phys. **59**, 113 (1964); A. J. Elwyn, J. E. Monahan, R. O. Lane, A. Langsdorf, Jr., and F. P. Mooring, Phys. Rev. **142**, 758 (1966).

relative to the incident protons. This partially polarized beam was then scattered from a slab-shaped sample of pile-grade graphite. The large face of the sample measured 9 in.×16 in., and its thickness was $\frac{1}{8}$ in. Neutrons scattered by the graphite were detected simultaneously at five angles as in previous measurements.[10] A transverse magnetic field between the neutron source and the scatterer precessed the spins of the neutrons through 180°. Measurements with this magnetic field off, and then on, gave (in the usual way) the product of the polarizations produced by the source and scattering interactions.

Multiple-scattering corrections to $\sigma(\theta)$ were made by use of a Monte Carlo program.[16] The polarization data also were corrected approximately for multiple scattering as described previously.[11,15] At all energies above 0.7 MeV, the transmission of the sample was greater than 90%, so that the multiple-scattering effects were kept small. Corrections for the second group of neutrons were based on the fact that this group is
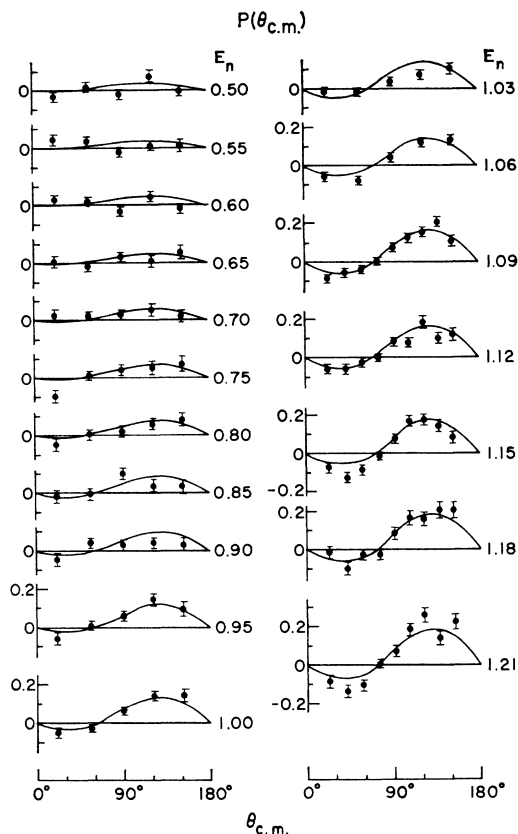

FIG. 1. Polarization of neutrons scattered from ¹²C. The neutron energy E_n is in MeV in the laboratory system, and the angle of scattering is in the c.m. system. The solid curves, the results of the R-function formalism, were calculated by use of the parameters of Table I.

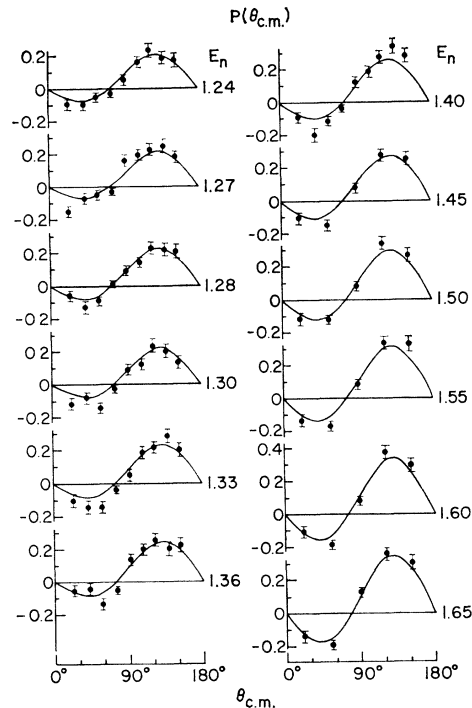[16] R. O. Lane and W. F. Miller, Nucl. Instr. Methods **16**, 1 (6262).

FIG. 2. Polarization of neutrons scattered from ¹²C. The neutron energy E_n is in MeV in the laboratory system, and the angle of scattering is in the c.m. system. The solid curves, the results of the R-function formalism, were calculated by use of the parameters of Table I.

unpolarized.[17] Since the minor isotope ¹³C has only 1.11% abundance, no correction for it was made, and within the accuracy of this experiment the results may be taken as those for ¹²C alone. The data were corrected for the known energy dependence of the efficiency[10] of each detector. The energy spread of the beam (produced mainly by the thickness of the Li target) was 25–50 keV. Because of the very slow variation of cross section with energy below 2.0 MeV, no correction for energy resolution was necessary. Since the first excited state in ¹²C is at 4.4 MeV, all scattering by ¹²C in this region is elastic.

III. EXPERIMENTAL RESULTS

Figures 1–3 show the experimental angular distributions of $P(\theta)$ at 0.5–2.0 MeV. Below 0.5 MeV, $P(\theta)$ is virtually zero. Values of the polarization for the ⁷Li(p, n)⁷Be reaction taken from Ref. 11 were used to derive $P(\theta)$ from the measured product of $P(\theta)$ and the source polarization.

At each energy, measurements were made at either 5 or 9 angles. The shapes of the angular distributions

[17] G. L. Morgan, C. E. Hollandsworth, and R. L. Walter, in *Proceedings of the Second International Symposium on Polarization Phenomena of Nucleons, Karlsruhe, 1965*, edited by P. Huber and H. Schopper (Birkhauser Verlag, Stuttgart, Germany, 1966), p. 523.
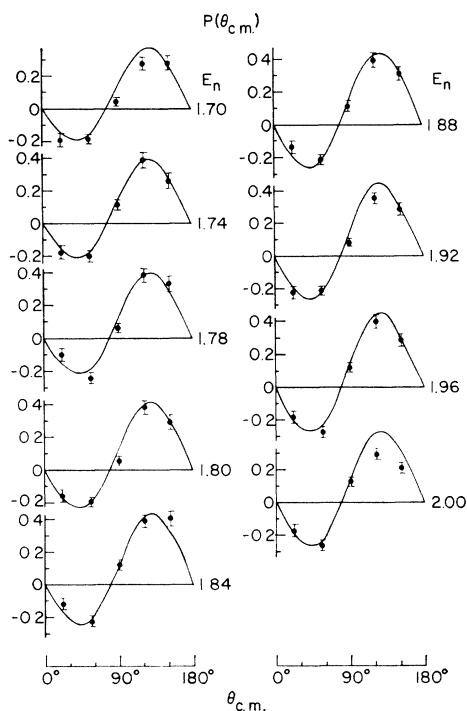
FIG. 3. Polarization of neutrons scattered from ^{12}C. The neutron energy E_n is in MeV in the laboratory system, and the angle of scattering is in the c.m. system. The solid curves are results of the R-function formalism and were calculated by use of the parameters of Table I.

are sufficiently simple that 5 angles are adequate even at the highest energy. The errors in $P(\theta)$ are chiefly statistical, as can be seen from the random fluctuations of the data about the solid curves as shown in Fig. 1–3. These solid curves represent the results of an R-function calculation to be discussed later. Beginning at approximately 0.7 MeV, a definite pattern of polarization (a combination of $\sin\theta$ and $-\sin2\theta$) appears. At high energies, the term in $-\sin2\theta$ is stronger. These results are in agreement with our earlier survey work[11] at two forward angles, 45°(lab) and 90°(lab), obtained without a spin-precession magnet. The results are also in agreement with some recent results[18] obtained with a spin-precession magnet. From the data, it can be seen that $P(\theta)$ reaches as high as 40% at back angles.

Figure 4 contains all the differential-cross-section results in the form of the coefficients B_L for the Legendre-polynomial expansion for $\sigma(\theta)$. The data below 0.5 MeV are from an earlier experiment.[10] The counts from the detectors were converted to cross section by normalizing $4\pi B_0$ to the known total scattering cross section[19] for carbon. This is done in the process of

---

[18] O. Aspelund (private communication).

[19] J. R. Stehn, M. D. Goldberg, B. J. Magarno, and R. Wiener-Shasman, in *Neutron Cross Sections*, compiled by O. J. Hughes and R. B. Schwartz (U. S. Government Printing Office, Washington, D.C., 1964), 2nd ed., Suppl. No. 2.

fitting an expansion of Legendre polynomials to the data in the c.m. system at each energy. Coefficients B_L for $L \geq 3$ are negligible below 2 MeV.

Figure 5 shows the energy dependence of the coefficients C_L in the associated Legendre-polynomial expansion for $\sigma_p(\theta) \equiv P(\theta)\sigma(\theta)$. The error bars are larger here because of the effect of the larger statistical errors on $P(\theta)$. Coefficients C_L for $L \geq 3$ are negligible below 2 MeV.

Experimental values of $\sigma(\theta)$ in the neighborhood of the $\frac{5}{2}^+$ resonance at 2.08 MeV have been reported previously[10] and are shown in Fig. 6 to complete the comparison between experiment and our R-function calculations.

IV. R-FUNCTION FITTING

The elastic scattering of neutrons from zero-spin nuclei is, in principle at least, one of the simpler cases for the application of the R-matrix theory. Since ^{12}C has zero spin, only one channel spin $(S=\frac{1}{2})$ is present, and for neutron energies below $E_n \approx 4.4$ MeV, only elastic scattering is possible and capture is negligible compared to scattering below 2 MeV. Thus there is
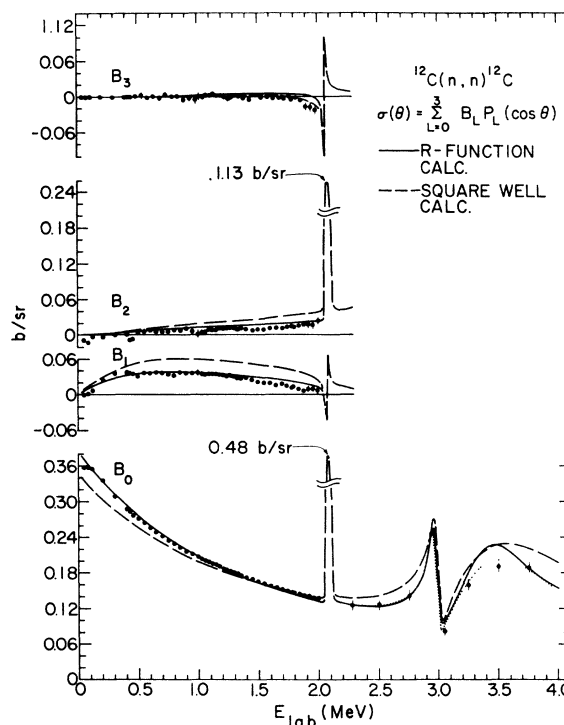

FIG. 4. Legendre-polynomial coefficients in the expansion of the differential scattering cross section for ^{12}C$+n$. Cross section and angles are in the c.m. system. Neutron energy is in the laboratory system. Data points for $E \leq 2$ MeV are from the present work. Data points for B_0 at $E > 2$ MeV are from Ref. 9 while the dotted curve is an average of data from Ref. 17. The calculated results for the 2.08-MeV resonance are shown here as the broken curves. Solid curves are calculated results of the R-function fitting and dashed curves are calculated results from the potential analysis using parameters of Table I. Where error bars are not shown, the error is represented by the size of the points.

effectively only one open channel in the energy interval of interest, and since the nearest closed channel is at 4.4 MeV, the R matrix can be approximated by an R function. The two $d_{3/2}$ resonances at 2.95 and 3.5 MeV are close together and interfere violently with one another as is seen from the total cross-section measurements. This degree of interference between "resolved" states of the same J^π is unusual in fast-neutron spectroscopy and requires the use of at least a two-level R function to represent these states that make a large contribution to the polarization below 2 MeV. A program COMBO[20] was written to calculate $\sigma(\theta)$, $P(\theta)$, B_L, and C_L from R-function parameters. The R function
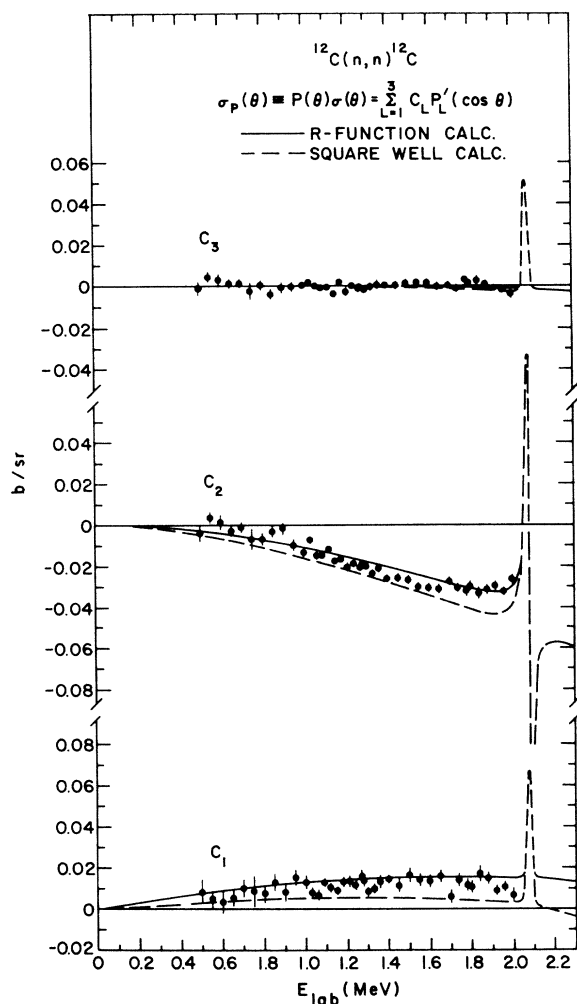

FIG. 5. Associated-Legendre-polynomial coefficients in the expansion of the polarized cross section $\sigma_p(\theta)$ for ^{12}C$+n$. Cross section and angles are in the c.m. system. Neutron energy is in the laboratory system. Solid curves are the calculated results of the R-function fitting and dashed curves are calculated results from the potential analysis using parameters of Table I.

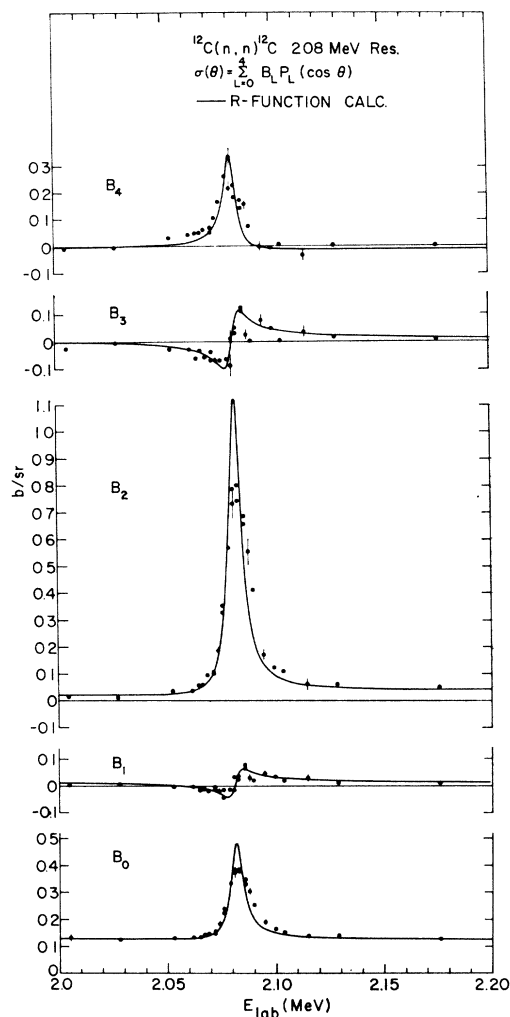[20] B. J. Raz and C. K. Bockelman, in Brookhaven National Laboratory Report No. BNL-9108, 1965 (unpublished).

FIG. 6. Legendre-polynomial coefficients in the expansion of the differential scattering cross section for ^{12}C$+n$ at the 2.08-MeV resonance. Cross section and angles are in the c.m. system. Neutron energy is in the laboratory system. The data points are from Ref. 10. The solid curve represents the results of the calculations with parameters of Table I.

used was

$$R_{lJ}(E) = \sum_{\lambda=1}^{2} \left[\frac{\gamma_\lambda^2}{E_\lambda - E} \right]_{lJ} + R_{lJ}{}^0, \qquad (1)$$

where γ_λ^2 and E_λ are the reduced width and characteristic energy, respectively, for the λth state of given J^π, and $R_{lJ}{}^0$ is the corresponding constant background term. The corresponding phase shift is

$$\delta_{lJ}(E) = \tan^{-1}\left(\frac{P_l(\rho) R_{lJ}(E)}{1 - (S_l - b_{lJ}) R_{lJ}(E)} \right) - \phi_l(\rho), \qquad (2)$$

where $P_l(\rho)$ is the penetration factor, $(S_l - b_{lJ})$ is the shift factor for boundary value b_{lJ}, the term $\phi_l(\rho)$ is the hard-sphere phase, and $\rho = kA$ with k the wave number and A the interaction radius. From these phase shifts, the quantities $B_L(E)$, $C_L(E)$, $\sigma(\theta, E)$, and $P(\theta, E)$ are

calculated over the energy range of interest according to the formulations of Blatt and Biedenharn,[21] and of Simon and Welton.[22] Values of $P_l(\rho)$, $S_l(\rho)$, and $\phi_l(\rho)$ have been tabulated.[23]

It is clear that the low-energy data are dominated by s waves, with a large contribution from the $s_{1/2}$ state in ^{13}C at $E_{ex}=3.09$ MeV, which is bound by approximately 1.86 MeV. The s-wave phase shift was obtained from a phase-shift analysis of the data for $\sigma(\theta)$ below 0.8 MeV in terms of s and p waves. Equally good fits of the effective range expansion

$$k \cot\delta_{0\frac{1}{2}} = -\alpha + \tfrac{1}{2}r_0 k^2 - \rho r_0^3 k^4 + \cdots \qquad (3)$$

to the data were obtained for a certain range of values for the parameters α, r_0, and ρ, where k is the momentum wave number, $1/\alpha$ the scattering length, r_0 the effective range, and ρ the shape parameter. Also included in the data for fitting were the zero-energy neutron scattering cross section[3,19] and the energy of the bound $s_{1/2}$ state. Values of ρ found from the fitting were very small, as expected at these energies, and ρ was set equal to zero in the subsequent analysis.

The effective-range parameters for $l=0$ neutrons and the boundary condition $b_{lJ}=0$ are related to the R-function parameters through the expressions

$$1/\alpha = A(1-R_{0\frac{1}{2}}^{(0)}), \qquad (4)$$

$$r^0 = 2[A - A^2\alpha + \tfrac{1}{3}(A^3\alpha^2) - (\hbar^2 A\alpha^2/2\mu)R_{0\frac{1}{2}}^{(1)}], \qquad (5)$$

where μ is the reduced mass and

$$R_{0\frac{1}{2}}^{(0)} = R_{0\frac{1}{2}}\big|_{E=0} \quad \text{and} \quad R_{0\frac{1}{2}}^{(1)} = dR_{0\frac{1}{2}}(E)/dE \big|_{E=0}.$$

The R-function parameters $\gamma_{0\frac{1}{2}}^2$, $E_{0\frac{1}{2}}$, and A were extracted from the effective-range parameters α, r_0, and the binding energy (B.E.) by the above relations together with the relation

$$R_{0\frac{1}{2}}(E)\big|_{E=\text{B.E.}} = -1/|kA|, \qquad (6)$$

which is the resonance condition for the bound state. Substituting a given set of values of α and r_0, together with B.E. $= -1.86$ MeV into Eqs. (4)–(6) gives a set of three nonlinear equations in $\gamma_{0\frac{1}{2}}^2$, $E_{0\frac{1}{2}}$, and A. These equations were solved for the R-function parameters by a gradient technique. The boundary value was $b_{0\frac{1}{2}}=0$.

The resulting R-function parameters depend quite sensitively upon α, r_0, and B.E. through Eqs. (4)–(6) so that this calculation is probably best employed as a consistency requirement on any set of R-function parameters rather than as a definitive method to obtain them. From the several sets of consistent R-function parameters obtained from the different but equally good effective-range fits, the set of effective-range parameters selected was $(1/\alpha)=6.14$ F, $r_0=3.367$ F.

The corresponding R-function parameters were $\gamma_{0\frac{1}{2}}^2=4.0$ MeV, $E_{0\frac{1}{2}}=-6.0$ MeV, and $A=3.72$ F. These effective-range parameters are generally consistent with those obtained by other groups.[5,12] This choice was based also on external considerations. Some of the effective-range fits led to values of A as large as 4.9 F. With such large values of the interaction radius, however, the p-wave interference effects due to the large phase angle ϕ_1 were almost an order of magnitude higher than the experimental effect (Fig. 4), especially above $E_n\approx0.5$ MeV. To remove this discrepancy, ϕ_1 could be reduced arbitrarily, or very large positive $R_{1\frac{1}{2}}^0$ and $R_{1\frac{3}{2}}^0$ could be assumed to give the p phases ϕ_1 required by the data. Neither of these alternatives seems justified. Some effective-range fits led to values of A somewhat less than 3.72 F. However, the corresponding values of $\gamma_{0\frac{1}{2}}^2$ considerably exceed the value $\tfrac{3}{2}\hbar^2/\mu A^2=4.87$ MeV, an upper limit to the single-particle estimate. Thus, by applying these additional external conditions, the above set of consistent parameters was chosen as an over-all best choice. The value of $\gamma_{0\frac{1}{2}}^2$ is expected to be large, since this is believed to be a single-particle state. These values of $\gamma_{0\frac{1}{2}}^2$ and $E_{0\frac{1}{2}}$ in terms of a potential model will be interpreted in the next section.

Since there are no broad p resonances near the region covered in this experiment, the contribution from such states was included as constant background terms, $R_{1\frac{1}{2}}^0$ and $R_{1\frac{3}{2}}^0$. The fact that C_1 is nonzero implies that $\delta_{1\frac{1}{2}}\neq\delta_{1\frac{3}{2}}$, and therefore $R_{1\frac{1}{2}}^0\neq R_{1\frac{3}{2}}^0$. The values that gave the best over-all fit were $R_{1\frac{1}{2}}^0=0.10$ and $R_{1\frac{3}{2}}^0=0.25$. The two $d_{3/2}$ resonances at laboratory energies of 2.95 and 3.52 MeV have a large effect on the polarization below 2 MeV. Therefore, a fit to the total cross section over these resonances was made to determine the R-function parameters $\gamma_{2\frac{3}{2}}^2$ and $E_{2\frac{3}{2}}$ for each of them. The level parameters that give the best fit to B_0 over these resonances are given in Table I and the corresponding calculated B_0 is shown in Fig. 4. Earlier preliminary calculations[14] did not include the effects of the bound $d_{5/2}$ state, which shows a large stripping width.[24] Subsequent interpretations in terms of a square well (Sec. V) showed that its effect at higher energies was indeed considerable. It was found that a constant $R_{2\frac{5}{2}}^0=-0.558$ was able to account for the effects of this bound state at laboratory energies up to 2 MeV. The $d_{5/2}$ scattering resonance at 2.076 MeV was included specifically as a level in the R function. The contribution of f waves was included only as hard-sphere scattering. No higher partial waves were calculated.

The final set of R-function parameters used is shown in Table I for physical boundary conditions b_{lJ} such that $E_\lambda\approx E_{\text{res}}$ for resonances near the energy region of the experiment. The corresponding calculated cross sections and polarizations are shown as the solid lines

[21] J. M. Blatt and L. C. Biedenharn, Rev. Mod. Phys. **24**, 258 (1952).

[22] A. Simon and T. A. Welton, Phys. Rev. **90**, 1036 (1953).

[23] J. E. Monahan, L. C. Biedenharn, and J. P. Schiffer, Argonne National Laboratory Report No. ANL-5846, 1958 (unpublished).

[24] T. S. Green and R. Middleton, Proc. Phys. Soc. (London) **A69**, 28 (1956).

TABLE I. R-function parameters for ^{12}C$+n$ with an interaction radius $A = 3.72$ F. The parameters shown are for physical boundary conditions b_{lJ} such that the E_λ fall near the observed resonance energies. The parameters in the upper half of the Table were used to calculate the solid curves of Figs. 1–6. The parameters in the lower half were used to calculate the dashed curves of Figs. 4 and 5.

lJ	$\lambda = 1$ E_{lJ} (MeV, c.m.)	$\gamma_{lJ}{}^2$ (MeV, c.m.)	$\lambda = 2$ E_{lJ} (MeV, c.m.)	$\gamma_{lJ}{}^2$ (MeV, c.m.)	$R_{lJ}{}^0$	b_{lJ}
			R-function fitting parameters			
$0\frac{1}{2}$	-1.86	4.0	$\cdots$	$\cdots$	0	-1.035
$1\frac{1}{2}$	$\cdots$	$\cdots$	$\cdots$	$\cdots$	0.1	0
$1\frac{3}{2}$	$\cdots$	$\cdots$	$\cdots$	$\cdots$	0.25	0
$2\frac{3}{2}$	2.734	0.212	3.372	1.742	0.107	-1.368
$2\frac{5}{2}$	$\cdots$	$\cdots$	1.922	0.030	-0.558	-1.541
		Square-well potential parameters for single-particle states				
$0\frac{1}{2}$	-1.866	2.994	$\cdots$	$\cdots$	0.0374	-1.072
$1\frac{1}{2}$	-22.78	4.42	25.75	3.43	0.084	0
$1\frac{3}{2}$	-27.30	4.42	21.24	3.43	0.086	0
$2\frac{3}{2}$	2.740^{a}	0.265^{a}	3.755	3.696	0.107	-1.368
$2\frac{5}{2}$	-3.303	3.684	1.914^{a}	0.037^{a}	0.112	-1.541

[a] Parameters of compound states that have been added to the R function generated from a square-well potential.

in Figs. 1–6. The agreement with the data is reasonably good over the entire interval $0.1 \leq E_n \leq 2.2$ MeV.

No polarization data on the narrow $d_{5/2}$ resonance at 2.076 MeV are available for comparison with the calculation. Figure 6 shows the comparison with the available data[10] for $\sigma(\theta)$, obtained with an energy spread approximately equal to the width of the resonance. This spread accounts for nearly all the systematic discrepancies between the data and the calculated curve. The measured width of the resonance was assumed in the calculations to be approximately 7 keV, as given in Ref. 9. The slight upward displacement of the laboratory resonance energy (2.082 MeV for the present data, 2.076 MeV for Ref. 9) is caused mostly by the skewing toward lower energies in the energy-spread distribution of the present data, so there is no real discrepancy between these two experiments. The resonances reported[25] near 2.8 MeV are extremely narrow and were neglected in these calculations.

The recent coupled-channel calculations of Reynolds *et al.*[26] give slightly smaller polarizations than those of the present R-function fit but the results of the two calculations are not inconsistent with each other.

V. INTERPRETATION OF RESULTS IN TERMS OF A SQUARE WELL

As was discussed previously, much of the neutron scattering from ^{12}C is dominated by the $s_{1/2}$ state in ^{13}C

(binding energy $= 1.86$ MeV) and the $d_{3/2}$ resonance at 3.52 MeV laboratory energy. The reduced widths of these states are relatively large. As a consequence, they are usually called single-particle states. Since another $d_{3/2}$ resonance occurs close to the one at 3.52 MeV, there is undoubtedly some mixing of higher-order configurations in these states. However, because the reduced width needed to fit the data is so large, it is probably safe to say that the single-particle component is the dominant one. To the extent that these states can be considered to be single-particle states, they can be described by a potential-well model. Thus, in the problem at hand, much of the scattering can be described as potential scattering. In order to see if this picture is consistent, R-function parameters for potential scattering were obtained by considering a square well, chosen because of the ease in obtaining solutions. While it is known that (because of its sharp edge) a square well does not completely reproduce potential scattering, it was felt that this potential could be used to estimate the anomalous background effects caused by the non-normal-parity states in ^{13}C below the neutron threshold and by the unobserved resonances that occur above the neutron-angular-momentum barrier.

The square well potential used is

$$V(r) = -V_0 + Cl^2 - V_{so}\boldsymbol{\sigma}\cdot\mathbf{l} \quad \text{for} \quad r < A,$$
$$= 0 \quad \text{for} \quad r > A,$$

where the strength V_{so} of the spin-orbit potential was taken as constant. The operator Cl^2 was included to give the proper spacing of the single-particle levels for different values of l. There are four parameters appearing, namely, V_0, C, V_{so}, and A. A was chosen to be

[25] S. Cierjacks, P. Forti, D. Kopsch, L. Kropp, and J. Nebe, in Proceedings of the Second Conference on Neutron Cross Sections and Technology, Washington, D.C., paper E-9 (unpublished); R. B. Schwartz, R. A. Schrack, and H. T. Heaton, *ibid.*, paper E-12.

[26] J. T. Reynolds, C. J. Slavik, C. R. Lubitz, and N. C. Francis, Phys. Rev. **176**, 1213 (1968).

3.72 F to be consistent with the analysis previously discussed. This left three parameters to be determined. These were found by assuming that the $\frac{1}{2}^+$ state with 1.86 MeV binding energy, the $\frac{5}{2}^+$ state bound by 1.10 MeV, and the $\frac{3}{2}^+$ level at 3.52 MeV laboratory energy were, respectively, the $2s_{1/2}$, $1d_{5/2}$, and $1d_{3/2}$ single-particle states. The potential parameters found are $V_0 = 41.3$ MeV, $C = 1.63$ MeV, and $V_{so} = 1.51$ MeV.

Using these parameters, we generated wave functions and R-function levels. Enough levels were generated so that the cross section obtained from the R-function expansion agreed to four significant figures with the exact potential scattering. To satisfy this condition, it is necessary to consider 20 levels for s and p waves and 19 levels for d waves. The reduced widths were then calculated. The level energies and reduced widths found for the single-particle states are -1.866 and 2.99 MeV for the $2s_{1/2}$ state, -3.03 and 3.68 MeV for the $1d_{5/2}$ state, and 3.755 and 3.70 MeV for the $1d_{3/2}$ state.

In most cases, no more than two R-function levels gave contributions that varied appreciably with neutron energy between 100 keV and 4 MeV. Thus, R_{lJ} was represented by up to two levels plus a background term R_{lJ}^0. The background term R_{lJ}^0 in Eq. (1) was estimated by removing those single-particle states shown in Table I from the R function, calculating the square-well R function with the remainder of the potential states for energies between 100 keV and 4 MeV in 100-keV steps, and then averaging these results. Since these remaining levels that contribute to the R function are relatively distant in energy, this approximation is very good. For the p states, the energy range of interest happened to lie approximately halfway between two potential R-function levels. In this case, these two levels were considered as the resonance terms and the remaining 18 levels were averaged over the energy range 100 keV–4 MeV. The parameters found are given in Table I.

This method of generating a background simulates the contribution from distant compound-nuclear states fairly well. As was shown by Lane, Thomas, and Wigner,[27] the compound-nuclear states are clustered about the single-particle states whose width W which is much less than the single-particle spacing D and much larger than the level spacing d in the region. Since W is of the order of a few MeV,[27] and since D is relatively large, the replacement of all these complex states by the single-particle state is probably a good approximation. However, states at a distance comparable to W should probably be included as individual states.

The $\frac{5}{2}^+$ resonance at $E_n = 2.076$ MeV and the $\frac{3}{2}^+$ resonance at $E_n = 2.95$ MeV are compound resonances, not potential resonances. Therefore, terms corresponding to these states were added to the corresponding potential R function, as indicated in Table I, to give

the total R function. This is an approximation in the sense that we are assuming that the single-particle states are eigenfunctions of the true Hamiltonian in the interior of the nucleus. This is obviously not the case for all the states—in particular, not for the $\frac{3}{2}^+$ state at 3.52 MeV. However, we make this approximation in an attempt to obtain order-of-magnitude estimates for the background term R_{lJ}^0. A more detailed structure calculation would be required to give a more nearly accurate picture of these states. The final parameters obtained from the potential analysis as well as the parameters of the added compound states are given in Table I, and the results calculated with these parameters are shown in Figs. 4 and 5. The fact that no change in the parameters of the $\frac{3}{2}^+$ compound resonance improved the fit indicates that the discrepancy between the calculated B_0 and the experimental values probably is the result of the assumptions that the $\frac{3}{2}^+$ state at 3.52 MeV is a single-particle state. In fact, if we take the ratio of the fitted reduced width to that of the reduced width for the potential scattering and call this the spectroscopic factor S of the state, we find $S = 0.47$.

The over-all fit is not too bad for such a simple potential. However, it is well known that a diffuse potential well is more representative of an average nucleon-nucleus interaction. Vogt[28] has shown that the use of a diffuse well is very important in such calculations. Calculations are now under way to examine these data by use of the method discussed here but with a Woods-Saxon potential.

Some method short of a complex structure calculation is needed to take into account the mixing of potential states into more complex states, as probably occurs for the two $d_{3/2}$ resonances at 2.95 and 3.52 MeV. Perhaps the method discussed by Schiffer[29] would be useful.

A comparison of the parameters for the two analyses (Table I) shows that the bound $\frac{1}{2}^+$ state in ^{13}C at 3.09 MeV is nearly pure single-particle. Because the only known p states in ^{13}C are rather distant from our energy region, only $R_{1\frac{1}{2}}^0$ and $R_{1\frac{3}{2}}^0$ background terms could meaningfully be extracted from these results. Evaluation of the total R functions for p-wave potential parameters at $E_n(c.m.) = 1$ MeV gives $R_{1\frac{1}{2}}(1 \text{ MeV}) \approx 0.05$ and $R_{1\frac{3}{2}}(1 \text{ MeV}) \approx 0.1$, which are slightly smaller than the values obtained by fitting the data. Comparison of the value of $\gamma_{2\frac{3}{2}}^2$ in Table I ($\lambda = 2$) for the assumed single-particle state in the potential analysis with the value of the corresponding reduced width from the fitting procedure shows that this state is not pure single-particle but contains mixing of higher-order configurations. As mentioned earlier, this was expected because of the proximity of another $\frac{3}{2}^+$ state. The bound single-particle $\frac{5}{2}^+$ state was found from the

[27] A. M. Lane, R. G. Thomas, and E. P. Wigner, Phys. Rev. **98**, 693 (1955).

[28] E. Vogt, Rev. Mod. Phys. **34**, 723 (1962).
[29] J. P. Schiffer, Nucl. Phys. **46**, 246 (1963).

potential analysis to have the parameters given in Table I under $\lambda = 1$. Evaluation of the R function for the potential parameters at $E_n = 2$ MeV (c.m.) gives $R_{2\frac{1}{2}}(2 \text{ MeV}) = -0.583$. Thus the background term assumed in the fitting provides a reasonable simulation of the sum of the resonance term and the background found from the potential analysis.

The results of these calculations would seem to indicate that the potential-well analysis used here is of value. By using this scheme, it would seem that background contributions can be reasonably well determined in an *a priori* manner and that only compound resonance parameters need be fitted. This eliminates several of the parameters needed in the fitting procedure and,

therefore, reduces somewhat the ambiguity of the parameters found. However, a diffuse-well calculation is expected to give better agreement with the data.

ACKNOWLEDGMENTS

Experimental Investigations of the C¹²(h, p)N¹⁴ Reaction Mechanism

F. Haas, B. Heusch, A. Gallmann, and D. A. Bromley*

Laboratoire de Physique Nucléaire et d'Instrumentation Nucléaire, Strasbourg, France

(Received 9 June 1969)

Systematic studies on proton angular distribution and proton–γ-radiation angular correlations have been carried out on the C¹²(h, p)N¹⁴ reaction throughout the energy range $4.62 \leq E_h \leq 11.0$ MeV. ($h \equiv$ He³.) Both direct and compound-system reaction amplitudes are present; however, the latter appear to dominate. Striking resonant phenomena are observed, and it is suggested that these correspond to quasigiant resonances in the excitation-energy range from 17 to 23 MeV in O¹⁵ having a particularly simple structure involving single-proton orbitals coupled to excited N¹⁴ core configurations. A systematic correlation has been observed between the population of $|m| = 1$ magnetic substates of the 7.03-MeV state in the residual nucleus and the appearance of backward peaking in the corresponding proton angular distributions. A crude argument relating these phenomena to the participation of a heavy-particle direct stripping mechanism is suggested.

I. INTRODUCTION

ALTHOUGH extensive studies have been reported (see Ref. 1 for a review of all work prior to 1960 and detailed references of this work) on the mechanism for reactions induced by He³ nuclei (henceforth *helions*, h)[2] on light nuclei, relatively little unambiguous information has been obtained. Even at low bombarding energies, the high helion mass excess (14.93 MeV) results in high compound-system energies, typically ~ 20 MeV, so that isolated compound-resonance phenomena are not anticipated: Moreover, it has been demonstrated that in many of the reactions studied, direct reaction amplitudes play an important, if not dominant, role.

Examination of the compound-system binding energies for helions incident on light targets[1] shows three

somewhat anomalous cases. In the Be⁷ compound system, the helion binding energy is only 1.58 MeV; at low helion energies, no compound states are accessible and the reaction proceeds by direct capture. In the Ne¹⁹ compound system, the helion binding energy is next lowest at 8.42 MeV; studies on this system, and particularly on the O¹⁶(h, α)O¹⁵ reaction, did successfully isolate and study resonances in the Ne¹⁹ system,[3] but to date this is the only such example in helion studies. The next lowest binding energy is that in O¹⁵ (12.12 MeV), corresponding to helion bombardment of a C¹² target. In the hope of finding a situation amenable to detailed reaction mechanism study at the relatively low energies ($E_h \lesssim 11$ MeV) available for this work, and on the basis of the availability of much previous data on this reaction from this laboratory, and elsewhere, we have concentrated on the C¹²(h, p)N¹⁴ interaction.

The earliest measurements on this reaction at low energies[4] demonstrated clearly that even for $E_h \leq 3$

* Permanent address: Wright Nuclear Structure Laboratory, Yale University, New Haven, Conn. 06520.

¹ D. A. Bromley and E. Almqvist, in *Reports on Progress in Physics* (The Physical Society, London, 1960), Vol. 23, p. 544ff. See this review for detailed referencing of all earlier work on helion reactions.

² See, for example, Proceedings of the Tokyo Symposium on Helium 3 Reactions, Tokyo, 1968, edited by K. Matsuda (unpublished).

³ D. A. Bromley, J. A. Kuehner, and E. Almqvist, Nucl. Phys. **13**, 1 (1959).

⁴ D. A. Bromley, E. Almqvist, H. E. Gove, A. E. Litherland, E. B. Paul, and A. J. Ferguson, Phys. Rev. **105**, 957 (1957).